RSC Advances

ROYAL SOCIETY OF CHEMISTRY

www.rsc.org/advances

Facile Synthesis of Biocompatible N, S-doped Carbon Dots for Cell Imaging and Ion Detecting

Yupeng Sun, Chen Shen, Jing Wang and Yun Lu*

Department of Polymer Science and Engineering, State Key Laboratory of Coordination Chemistry, Key Laboratory of High Performance Polymer Materials and Technology of Ministry of Education, School of Chemistry and Chemical Engineering, Nanjing University, Nanjing 210093, PR China

Abstract

A facile, simple, effective and green method has been developed to synthesize the nitrogen and sulfur co-doped carbon dots (N, S-CDs) from heparin sodium. The as-prepared N, S-CDs possess naked-eyes observable blue-green luminescence, good biocompatibility, low toxicity and strong fluorescence in live cell imaging, indicating their great potential served as high quality optical imaging probes. Besides, the N, S-CDs can also be used as a competitive fluorescent sensing platform for the detection of Fe^{3+}.

Introduction

Fluorescent carbon dots (CDs) have attracted tremendous attention since 2006[1] because of their appealing properties and wide applications in the field of bioimaging, photocatalysts, fluorescent probes, environmental testing, drug carriers and so on[2-9]. So far, there are mainly two types of routes to synthesize CDs: top-down[10-12] and bottom-up[13-15]. By comparison, the latter is more convenient via adjusting the composition and properties of CDs with the selection of various precursors and synthesis conditions[16]. On the other hand, heteroatom doping is often used to improve the optical and electrical properties of CDs due to its ability to change the electronic density of the system[17-19]. Recently, single nitrogen-doped (N-CDs) or sulfur-doped CDs (S-CDs) have caught much attention because the nitrogen atom has a comparable atomic size and five valence electrons to bind carbon atoms, and the sulfur atom could provide the density of states or emissive trap states for photoexcited electrons to modify the band-gap energy[3, 20-27], thus offering the functionalized CDs more optimized properties. Qian et al. synthesized a series of N-CDs with different nitrogen contents under a solvothermal treatment of CCl_4 and diamines and illustrated the correlation between quantum yield and nitrogen content[25]. Chen et al. fabricated nitrogen-rich quantum dots with 2-azidoimidazole, whose nitrogen content was as high as 34.48%[26]. Chandra et al. prepared S-CDs from thiomalic aicd for the fabrication of solar cell devices[23]. Hu et al.

synthesized S-CDs using waste frying oil and sulfuric acid, which showed a good pH-sensitive behavior[27]. For multi-heteroatom co-doped CDs, their fluorescence and absorption behaviors possibly result from the synergistic effect. In fact, some nitrogen and sulfur co-doped CDs (N, S-CDs) have been reported recently[16, 19, 28-34]. Dong et al. used citric acid and L-cysteine to fabricate N, S-CDs and provided deep insights to their photoluminescence enhancement mechanism[28]. Ding et al. employed α-lipoic acid and ethylenediamine to obtain N, S-CDs and compared the quantum yield among N-CDs, S-CDs and N, S-CDs[31]. Nevertheless, it is still a challenge to prepare N, S-CDs with novel properties using a single precursor under a facile and effective treatment.

In this work, a facile and simple strategy is developed for the hydrothermal synthesis of N, S-CDs by using heparin sodium as the precursor (Fig. 1). It is found that both nitrogen and sulfur element are doped in the carbon dots. The prepared N, S-CDs exhibit small particle size, quite low toxicity, excellent biocompatibility and good fluorescence feature, and have been successfully applied in live cell imaging and ion detecting.
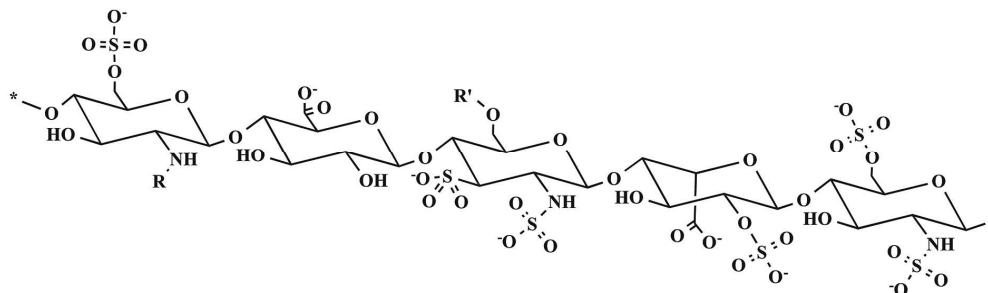
Fig. 1 Structure of heparin sodium.

Experimental Section

Chemicals and reagents

Heparin sodium with a molecular weight of 12000 was purchased from Aladdin Ltd. (Shanghai, China). All the other chemicals were purchased from Sigma-Aldrich (Shanghai, China) and used as received without further purification. Doubly deionized water prepared by a Milli-Q (MQ) water system was used throughout the experiments.

Synthesis of the N, S-CDs

The N, S-CDs were prepared by hydrothermal treatment of heparin sodium. The typical experimental procedure is described as follows: 0.25 g heparin sodium was dissolved in 20 mL

deionized water under agitation at room temperature, and then the solution was transferred to a stainless steel autoclave with a 25 mL Teflon liner and heated at 260 ºC for 12 h. After being cooled to room temperature naturally, the resulting yellow aqueous solution was centrifuged at 10000 rpm for 20 min to remove the non-fluorescent deposit. Next, the N, S-CDs solution was extracted with dichloromethane to discard the sodium salt due to the decomposition of heparin sodium. Finally, the N, S-CDs were obtained for further characterization after rotary evaporation from the dichloromethane solution and drying.

Characterization

Ultraviolet-visible (UV-Vis) absorption spectra were obtained using a UV-3600 spectrophotometer (Shimadzu). Fourier transform infrared (FT-IR) spectra were recorded on a Bruker VECTOR22 spectrometer using KBr pressed disks. X-ray diffraction (XRD) patterns were acquired on an XRD-6000 instrument (Shimadzu, Japan) with Cu Kα radiation source. X-ray photoelectron spectroscopy (XPS) analysis was performed on a PHI 5000 Versaprobe system, using monochromatic Al Kα radiation (1486.6 eV) operating at 25 W. Raman spectrum was recorded using a LabRAM Aramis laser confocal Raman spectrometer excited by 532 nm at ambient temperature. Elemental composition data was collected on a CHN-O rapid element analyzer (Heraeus, Germany). High-resolution transmission electron microscopy (HRTEM) images were taken using a JEOL 2010 electron microscope at an accelerating voltage of 200 kV. PL spectra were obtained on a steady-state fluorescence spectroscopy (Horiba Jobin Yvon FM-4NIR). Fluorescence lifetime was measured with a lifetime fluorescence spectroscopy (Horiba Jobin Yvon TemPro-01). Confocal images of the cells were acquired using a confocal microscope (LabRAM Aramis Horiba, Japan) with a laser excitation wavelength of 405 nm at room temperature.

Quantum yield calculations

The quantum yield of the N, S-CDs was calculated by measuring the fluorescence intensity in aqueous dispersion by using the following equation[35],

$$Q_{CD}=Q_R \cdot \frac{I_{CD}}{I_R} \cdot \frac{A_R}{A_{CD}} \cdot \frac{\eta_{CD}^2}{\eta_R^2}$$

Where Q is the quantum yield, I is the integrated intensity of luminescent spectra, A is the absorbance at exited wavelength, and η is the refractive index of the solvent used, using quinine sulfate (The quantum yield is 54%.) in 0.1 M H_2SO_4 solution as the reference. The subscripts CD

for carbon dots and R for reference are used in this equation.

Cellular toxicity test

The cytotoxicity of the N, S-CDs was evaluated by an AO/EB assay on acute HL-60 cells. Simply, 200 μL cell suspension was transferred to the each well of 96-well plate and cultured at 37 ℃ under 5% CO_2 in standard incubator for 12 hours and 24 hours after the addition of the N, S-CDs suspension with different concentrations. Then combined AO/EB staining was executed for cell state examination. 10 μL AO/EB (100 μg/mL) was added to each well. The resulting fluorescence images of the cells were monitored by the Leica DMIRE2 microscope fluorescence analyzing system. Cell viability data was captured by Nano Measurer program.

Cell imaging

HeLa cells were plated in a cover-glass-bottom dish in Dulbecco's Modified Eagle's Medium (DMEM) cell culture medium with 10% fetal bovine serum, 100 mg/L penicillin and 100 mg/L streptomycin. After incubation for 12 h, the cells were incubated with N, S-CDs at a concentration of 200 μg/mL. Then, the cells were washed with phosphate buffered saline (PBS) for three times to discard the redundant N, S-CDs. The images were taken by a confocal laser scanning microscope once the incubation and washing process were accomplished.

Metal ion detection

For the detection of various metal ions, NaCl, KCl, $AgNO_3$, $MgSO_4$, $CaCl_2$, $MnCl_2$, $FeSO_4$, $Co(NO_3)_2$, $NiCl_2$, $CuCl_2$, $ZnCl_2$, $Pb(NO_3)_2$, $AlCl_3$, $CrCl_3$ and $FeCl_3$, have been used as various ion sources. In a typical detection experiment, the solutions containing a calculated amount of ions were added into the N, S-CDs solution (0.001 g/L). After mixing evenly, the PL spectra were detected at 325 nm excitation. All of the experiments were performed in PBS buffer (pH = 6.86) unless stated otherwise.

Results and discussion

Heparin sodium with the sodium salt structure of a polysulfated polysaccharide is a natural anticoagulant material[36], and on complete hydrolysis, it liberates D-glucosamine, D-glucuronic acid, L-iduronic acid, acetic acid and sulphuric acid. In our case, under a hydrothermal condition, the carbon source heparin sodium could form directly the functionalized carbon dots after going through thermal condensation and carbonization without any additional or subsequent chemical modification. The oxygen-containing functional groups on the carbon dots confer a good

solubility in water[37], and the nitrogen- and sulfur-containing functional groups are expected to play the role of heteroatom doping to contribute the improved optical and electrical properties[16, 28]. The as-prepared N, S-CDs possess spherical structure with a mean diameter of 3.73 nm (Fig. 2a and 2b). High-resolution TEM (HR-TEM) reveals clear lattice fringes which should be attributed to sp^2 clusters in the N, S-CDs obtained via the hydrothermal route[38], suggesting the high crystallinity of the N, S-CDs. The lattice spacing distance is 0.24 nm, which is close to the (100) facet of graphene.
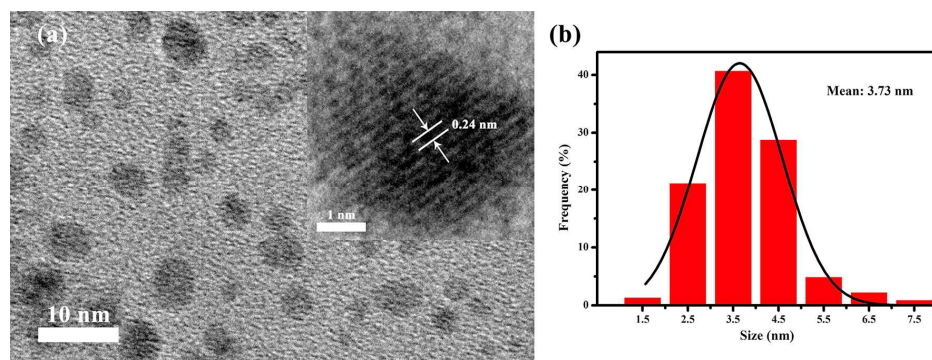

Fig. 2 (a) TEM image and the high magnification image (inset) of the N, S-CDs. (b) The corresponding size distribution histogram.

The functional groups of the N, S-CDs are characterized by FT-IR spectroscopy (Fig. 3a). The broad peak at about 3380 cm^{-1} is attributed to the O-H and N-H stretching vibration, indicating the presence of hydroxyl and amino groups[39], which contribute to the good hydrophilicity of N, S-CDs[16]. The band between 2810 cm^{-1} and 3000 cm^{-1} appears because of the C-H bonds, while a small peak observed at 2348 cm^{-1} corresponds to C-N and S-H bonds[19]. The peak at 1655 cm^{-1} and 1310 cm^{-1} is assigned to the COO^- groups and the small peak at 1560 cm^{-1} is ascribed to N-H bonds[38]. The peak at 1460 cm^{-1} can be identified as aromatic C=C bonds. Besides, there is a peak around 1060 cm^{-1}, which is due to C=S and S=O bonds[16].
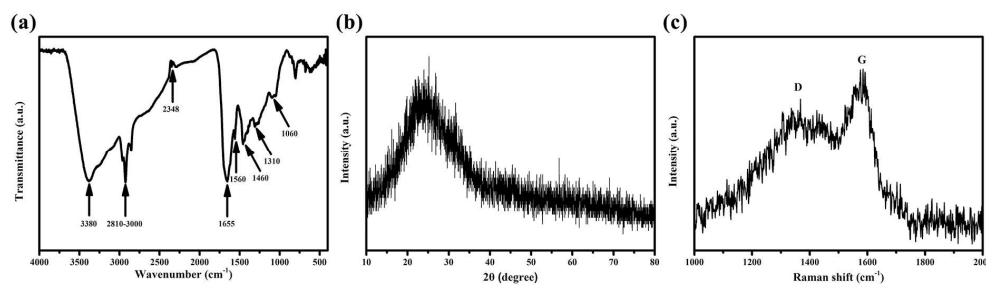
**Fig. 3 FT-IR spectrum (a), XRD pattern (b) and Raman spectrum (c) of the N, S-CDs.**

The XRD pattern shows a broad diffraction peak at 23.5º (Fig. 3b), indicating that the interlayer spacing of the (002) diffraction peak is 0.39 nm. The spacing is larger than that of graphite (0.34 nm), probably due to the introduction of nitrogen-, sulfur- and oxygen-containing groups[19]. Raman spectrum of the N, S-CDs is displayed in Fig. 3c. Two broad peaks around 1367 cm^{-1} and 1577 cm^{-1} are attributed to D and G bands related to the presence of sp^3 defects and the in-plane vibration of sp^2 carbon, respectively. The relative intensity of the disordered D band and the crystalline G band (I_D/I_G) can be used to correlate the structural properties of the carbon[16]. The I_D/I_G is 0.74 for the N, S-CDs, indicating the high crystallinity and graphitization of the N, S-CDs. XPS is used to investigate the elemental composition and oxidation states of the prepared N, S-CDs. In the full scan XPS spectrum of the N, S-CDs as shown in Fig. 4a, there are four peaks at 168 eV, 284 eV, 400 eV and 531 eV corresponding to S 2p, C 1s, N 1s and O 1s, respectively. Besides, the content of C, O, N and S elements gathered by element analysis is 56.73 wt%, 27.26 wt% (calculated), 5.49 wt% and 4.60 wt%, respectively, which indicates that the prepared carbon dots contain nitrogen and sulfur elements definitely. The high-resolution spectrum of C 1s displays five main binding energy peaks (Fig. 4b). The peaks at 284.4 eV and 285.0 eV confirm the graphitic structure (sp^2 C-C) and the C-H bonds in the N, S-CDs. The peak around 286.5 eV corresponds to C-O, while two peaks at 287.2 eV and 288.0 eV suggest the presence of C-S, C=O and C-N, respectively[40]. The high-resolution N 1s spectrum of the N, S-CDs shows two peaks (Fig. 4c) at 399.5 eV and 401.0 eV which are attributed to the pyrrolic N (C-N-C) and N-H bonds, respectively[41]. In the high-resolution spectrum of S 2p (Fig. 4d), there are three peaks at 163.4 eV, 164.2 eV and 168.6 eV, which correspond to S $2p_{3/2}$ and S $2p_{1/2}$ of thiophene S due to spin-orbit coupling[42] and the oxided S[43]. These results are consistent with the information offered from FT-IR spectrum.
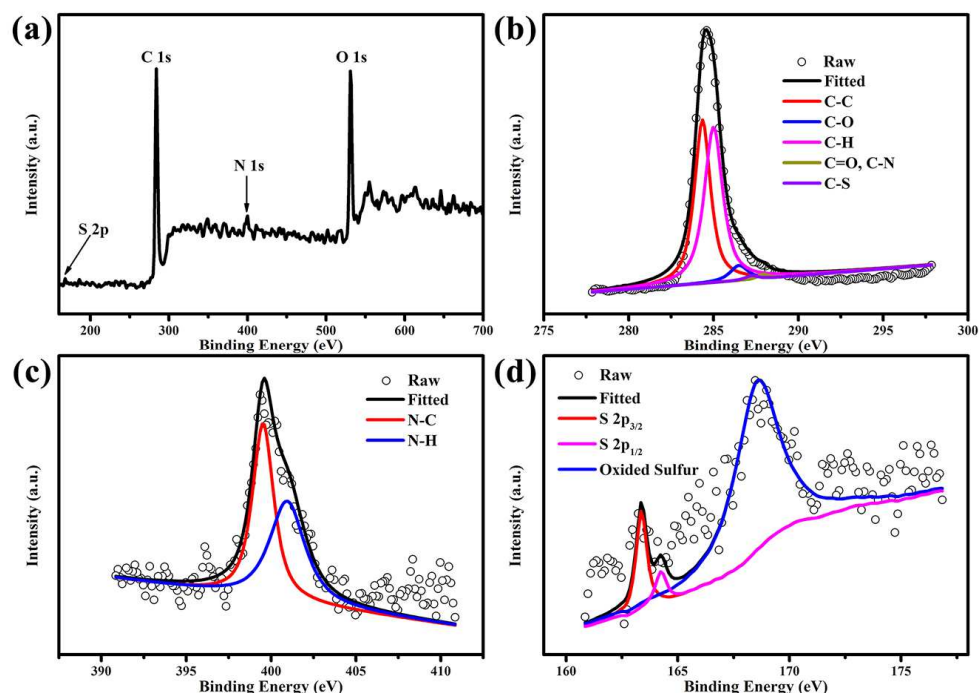
Fig. 4 (a) XPS full survey of the N, S-CDs. The high-resolution of C 1s (b), N 1s (c) and S 2p (d) spectra of the N, S-CDs.

The typical UV-Vis absorption spectrum of the N, S-CDs is displayed in Fig. 5a. The peak at 317 nm is attributed to the n-π* transition of the C=O bond[16, 44], confirming the existence of oxygen elements in the CDs. A shoulder peak is detected at 245 nm due to the π-π* transition of aromatic sp^2 domains[28, 45, 46]. It is worth noting that the N, S-CDs solution at a very low concentration is colorless, but displays the naked-eyes observable blue-green light under the illumination of UV (365 nm) light (inset in Fig. 5a). When the N, S-CDs are excited at 325 nm, a maximum emission intensity at 390 nm can be detected. Furthermore, the N, S-CDs exhibit an excitation-wavelength-dependent PL behavior, which is an intrinsic property of the carbon particles, as demonstrated in previous reports[47-49]. As they are excited at wavelength from 325 nm to 500 nm, the N, S-CDs emit at longer wavelength, displaying tunable emission properties (Fig. 5b). The quantum yield, for the N, S-CDs, using quinine sulfate as the reference is 7.41%, which is higher than the single nitrogen-doped CDs prepared from glycine[50] and sulfur-doped CDs prepared from waste frying oil[27]. It suggests that the synergic effects between nitrogen and sulfur atoms may enhance the effects of single nitrogen or sulfur atoms on the properties of CDs[33]. Fig. 5c shows the PL decay profiles of the N, S-CDs, recorded with excitation and emission wavelengths of 340 nm and 390 nm, respectively, at room temperature using a time-correlated

single photon counting technique. The fluorescence lifetime data of the N, S-CDs shows a multi-exponential function and average fluorescence lifetime is 4.73 ns. Such a short fluorescence lifetime revealed the radiative recombination nature of excitations[51].
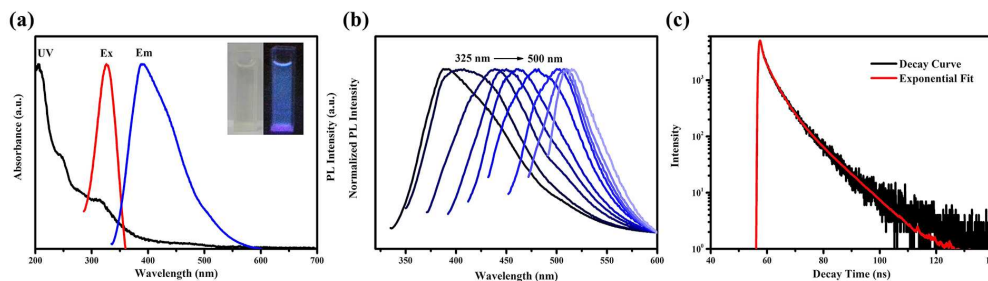
Fig. 5 (a) UV-Vis absorption spectrum, photoluminescence excitation and emission spectrum of the N, S-CDs aqueous solution (Inset: photographs taken under visible light (left) and 365 nm UV light (right), respectively). (b) The PL emission spectra of the N, S-CDs excited at wavelengths from 325 nm to 500 nm with the increment of 20 nm. (c) The PL decay curve and the exponential fitting curve of the N, S-CDs.

The effect of reaction temperature on the quantum yield of N, S-CDs is displayed in Table 1. The quantum yield increases from 1.23% to 7.41% as the temperature goes up from 120 ºC to 260 ºC. Therefore, 260 ºC is selected as the reaction temperature for preparing N, S-CDs.

Table 1 The relationship between reaction temperature and quantum yield.

Temperature (^{o}C)	120	140	160	180	200	220	240	260
Quantum Yield (%)	1.23	2.68	3.16	3.67	3.56	5.38	5.07	7.41

Carbon dots are usually used for cell imaging due to the good biocompatibility and obvious fluorescence, and the as-prepared N, S-CDs can be employed for this application as well. To verify the low cytotoxicity of the N, S-CDs, the AO/EB assay was carried out using acute HL-60 cells (Fig. 6d). The relative cell viability is 92.6% even after a 24 h exposure with a N, S-CDs concentration of 200 μg/mL, which is much better than that of CDs reported in the literature[19, 38, 52]. When the N, S-CDs are introduced into the HeLa cells for in vitro bioimaging as shown in Fig. 6, there is no change in the cell morphologies before and after incubation with the N, S-CDs, further indicating their low toxicity and good biocompatibility. The blue emissions from the N, S-CDs can be observed when excited at 405 nm. Notably, the fluorescent areas are mainly in the cytoplasm, particularly around the cell nucleus. Nevertheless, very weak PL intensity is detected in the cell

nucleus, suggesting that the N, S-CDs can penetrate into the cells easily but not into the nucleus. The phenomenon is consistent with the results on the interactions between carbon dots and viable cells in the previous reports[19, 53, 54], in which genetic disruption did not occur[4]. The very low toxicity and obvious fluorescence indicate that the N, S-CDs can be used as an excellent optical probe for cell imaging and other biomedical applications.
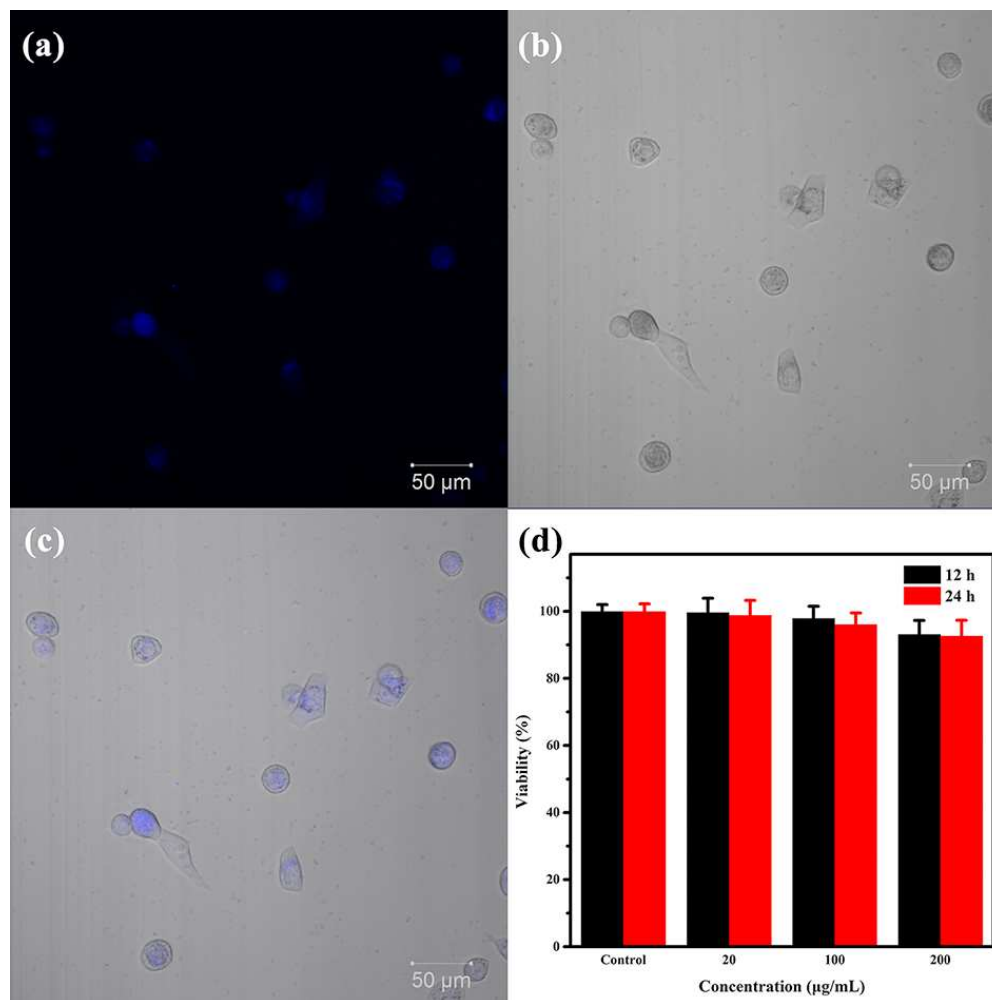
Fig. 6 Cellular imaging and cellular toxicity of the N, S-CDs. (a-c) Washed HeLa cells imaged under confocal fluorescent, bright field, overlap of corresponding bright field image and fluorescence image. (d) The effect of the N, S-CDs on the cells viability.

In addition, the as-prepared N, S-CDs can be applied in the detection of ferric ions. For the sake of the assessment of the selectivity of the N, S-CDs, the performance of the sensing system for various metal ions is investigated. Fig. 7 shows the PL spectra of N, S-CDs in the presence of representative metal ions including Na^+, K^+, Ag^+, Mg^{2+}, Ca^{2+}, Mn^{2+}, Fe^{2+}, Co^{2+}, Ni^{2+}, Cu^{2+}, Zn^{2+},

Pb^{2+}, Al^{3+}, Cr^{3+} and Fe^{3+} under identical conditions with a same concentration of 100 μM. A much lower PL intensity can be observed for the N, S-CDs due to the addition of Fe^{3+}, while no obvious decrease is seen after adding other metal ions into the N, S-CDs solution. This result indicates that the as-prepared N, S-CDs possess high selectivity for Fe^{3+}, and the other metal ions have a small impact on the sensing system. The high selectivity might be assigned to the high affinity between Fe^{3+} and the functional groups on the surface of N, S-CDs, especially the phenolic hydroxyl groups, which facilitated the aggregation of the N, S-CDs[2, 20, 31, 50, 55, 56]. The large N, S-CDs and Fe^{3+} aggregates are displayed obviously in TEM image (Fig. 8). In addition, fluorescence quenching may contribute to nonradiative electron-transfer that involves partial transfer of an electron in the excited state of the d orbital of ferric ion[2]. As shown in Fig. 9, there is no obvious change on the fluorescence spectra before and after adding EDTA into the N, S-CDs and Fe^{3+} solution, suggesting that the fluorescence quenching caused by Fe^{3+} is irreversible[57]. This further proves that the affinity between Fe^{3+} and the functional groups is very strong. The high sensitivity together with the high selectivity for Fe^{3+} makes the N, S-CDs a promising fluorescent sensing platform for the highly efficient detection of Fe^{3+}.
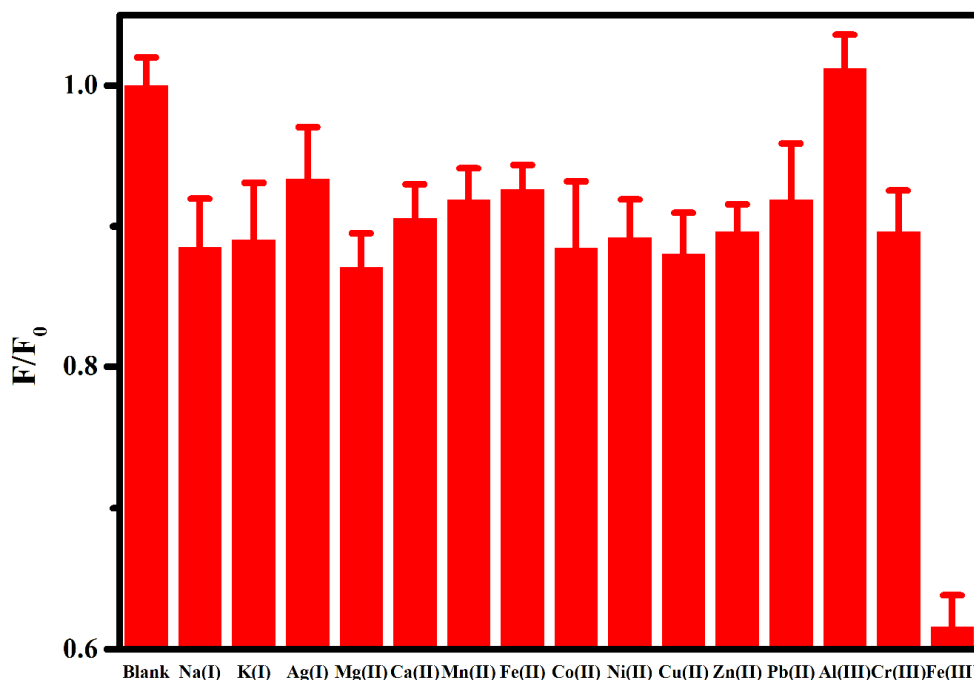
Fig. 7 The difference in photoluminescence intensity of N, S-CDs solution between the blank and solutions containing different metal ions (excitation at 325 nm; [M^{n+}] = 100 μM; pH = 6.86 in PBS buffer; F$_0$ and F are the photoluminescence intensities of the N, S-CDs at 390 nm

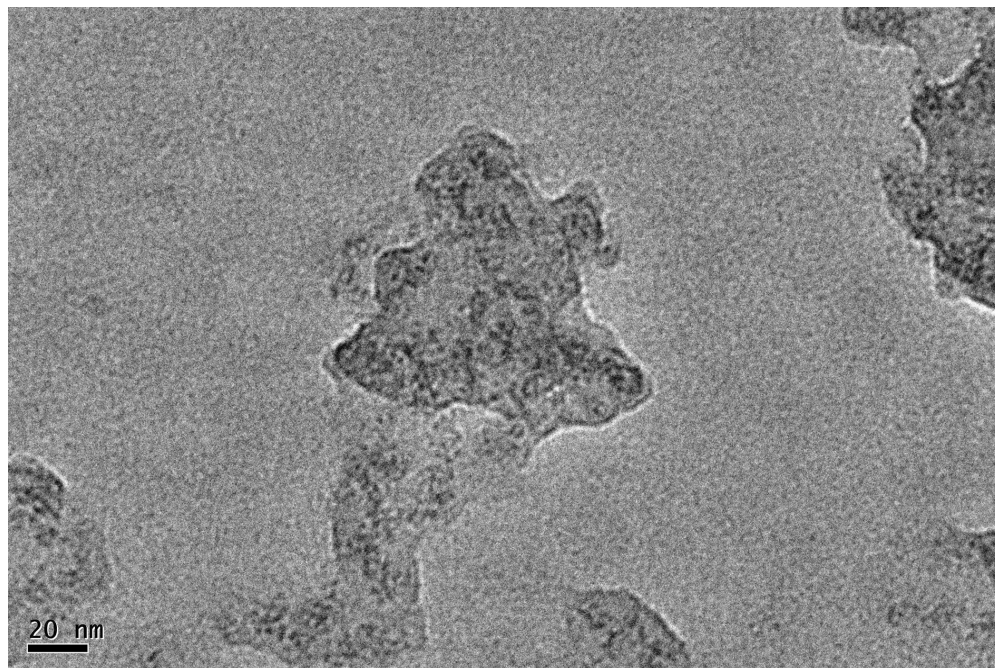in the absence and presence of ions, respectively).

Fig. 8 TEM image of the N, S-CDs and Fe^{3+} aggregates.
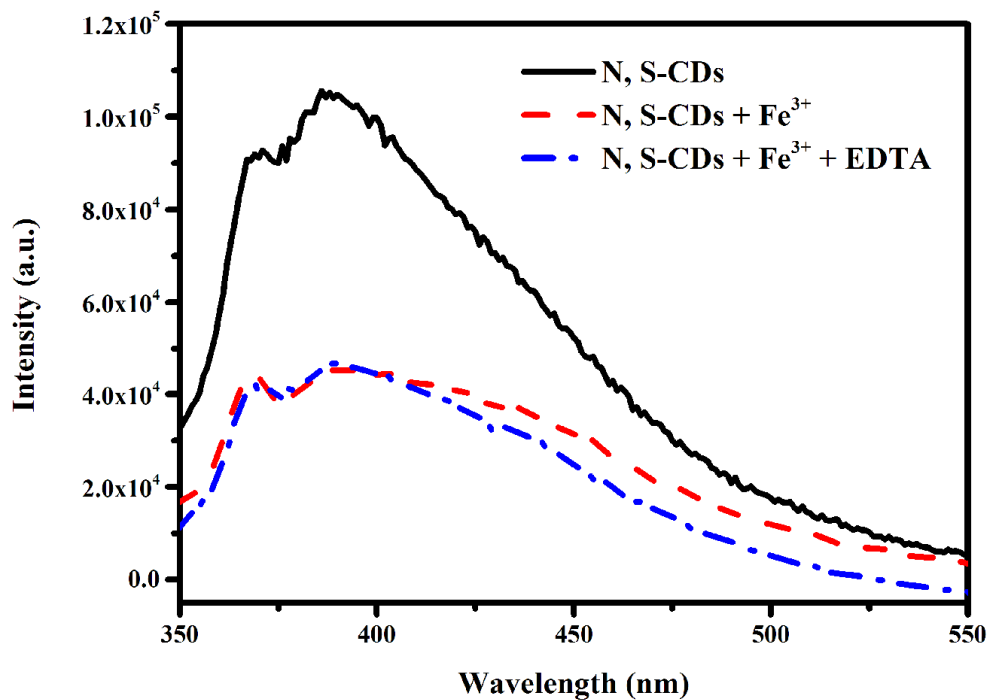

Fig. 9 Photoluminescence emission spectra of N, S-CDs (0.0001 g/mL), with addition of Fe^{3+}

(100 μM) and with the successive addition of EDTA (0.0001 M).

Conclusion

A facile, simple, effective and green method was developed to synthesize the nitrogen and sulfur

co-doped CDs by using heparin sodium as the precursor. The as-prepared water-soluble N, S-CDs exhibited strong blue-green fluorescence under UV illumination, which was closely dependent on the excitation wavelength. The cell viability was up to 92.6% even after a 24 h exposure with the N, S-CDs concentration of 200 μg/mL. Such a low toxicity and excellent biocompatibility indicate that the N, S-CDs have great potential in bioimaging and biolabeling. Furthermore, the N, S-CDs can also be used as a sensing platform for Fe^{3+} with high sensitivity and selectivity because their fluorescence can be strongly quenched by Fe^{3+}.

Acknowledgement

References

1. Y.-P. Sun, B. Zhou, Y. Lin, W. Wang, K. A. S. Fermando, P. Pathak, M. J. Meziani, B. A. Harruff, X. Wang, H. Wang, P. G. Luo, H. Yang, M. E. Kose, B. Chen, L. M. Veca and S.-Y. Xie, *J. Am. Chem. Soc.*, 2006, **128**, 7756-7757.

2. S. Zhu, Q. Meng, L. Wang, J. Zhang, Y. Song, H. Jin, K. Zhang, H. Sun, H. Wang and B. Yang, *Angew. Chem. Int. Ed.*, 2013, **52**, 3953-3957.

3. S. Liu, J. Tian, L. Wang, Y. Zhang, X. Qin, Y. Luo, A. M. Asiri, A. O. Al-Youbi and X. Sun, *Adv. Mater.*, 2012, **24**, 2037-2041.

4. F. Wang, Z. Xie, H. Zhang, C.-Y. Liu and Y.-G. Zhang, *Adv. Funct. Mater.*, 2011, **21**, 1027-1031.

5. H. Li, R. Liu, S. Lian, Y. Liu, H. Huang and Z. Kang, *Nanoscale*, 2013, **5**, 3289-3297.

6. H. Zhang, H. Huang, H. Ming, H. Li, L. Zhang, Y. Liu and Z. Kang, *J. Mater. Chem.*, 2012, **22**, 10501-10506.

7. C.-W. Lai, Y.-H. Hsiao, Y.-K. Peng and P.-T. Chou, *J. Mater. Chem.*, 2012, **22**, 14403-14409.

8. L. Zhou, Z. Li, Z. Liu, J. Ren and X. Qu, *Langmuir*, 2013, **29**, 6396-6403.

9. C. Shen, Y. Sun, J. Wang and Y. Lu, *Nanoscale*, 2014, **6**, 9139-9147.

10. L. Cao, X. Wang, M. J. Meziani, F. Lu, H. Wang, P. G. Luo, Y. Lin, B. A. Harruff, L. M. Veca, D. Murray, S.-Y. Xie and Y.-P. Sun, *J. Am. Chem. Soc.*, 2007, **129**, 11318-11319.

11. L. Zheng, Y. Chi, Y. Dong, J. Lin and B. Wang, *J. Am. Chem. Soc.*, 2009, **131**, 4564-4565.

12. D. Pan, J. Zhang, Z. Li and M. Wu, *Adv. Mater.*, 2010, **22**, 734-738.

13. L. Tang, R. Ji, X. Cao, J. Lin, H. Jiang, X. Li, K. S. Teng, C. M. Luk, S. Zeng, J. Hao and S. P. Lau, *ACS Nano*, 2012, **6**, 5102-5110.

14. H. Liu, T. Ye and C. Mao, *Angew. Chem. Int. Ed.*, 2007, **46**, 6473-6475.

15. R. Liu, D. Wu, S. Liu, K. Koynov, W. Knoll and Q. Li, *Angew. Chem. Int. Ed.*, 2009, **48**, 4598-4601.

16. D. Qu, M. Zheng, P. Du, Y. Zhou, L. Zhang, D. Li, H. Tan, Z. Zhao, Z. Xie and Z. Sun, *Nanoscale*, 2013, **5**, 12272-12277.

17. L. Tang, R. Ji, X. Li, K. S. Teng and S. P. Lau, *J. Mater. Chem. C*, 2013, **1**, 4908-4915.

18. L. Zhang and Z. Xia, *J. Phys. Chem. C*, 2011, **115**, 11170-11176.

19. D. Sun, R. Ban, P.-H. Zhang, G.-H. Wu, J.-R. Zhang and J.-J. Zhu, *Carbon*, 2013, **64**, 424-434.

20. A. Zhao, C. Zhao, M. Li, J. Ren and X. Qu, *Anal. Chim. Acta*, 2014, **809**, 128-133.

21. W. Wang, Y. C. Lu, H. Huang, J. J. Feng, J. R. Chen and A. J. Wang, *Analyst*, 2014, **139**, 1692-1696.

22. J. Xu, Y. Zhou, S. Liu, M. Dong and C. Huang, *Anal. Methods*, 2014, **6**, 2086-2090.

23. S. Chandra, P. Patra, S. H. Pathan, S. Roy, S. Mitra, A. Layek, R. Bhar, P. Pramanik and A. Goswami, *J. Mater. Chem. B*, 2013, **1**, 2375-2382.

24. W. Kwon, J. Lim, J. Lee, T. Park and S.-W. Rhee, *J. Mater. Chem. C*, 2013, **1**, 2002-2008.

25. Z. Qian, J. Ma, X. Shan, H. Feng, L. Shao and J. Chen, *Chem. Eur. J.*, 2014, **20**, 2254-2263.

26. X. Chen, Q. Jin, L. Wu, C. Tung and X. Tang, *Angew. Chem. Int. Ed.*, 2014, **53**, 12542-12547.

27. Y. Hu, J. Yang, J. Tian, L. Jia and J.-S. Yu, *Carbon*, 2014, **77**, 775-782.

28. Y. Dong, H. Pang, H. B. Yang, C. Guo, J. Shao, Y. Chi, C. M. Li and T. Yu, *Angew. Chem. Int. Ed.*, 2013, **52**, 7800-7804.

29. W. Wang, Y. C. Lu, H. Huang, A. J. Wang, J. R. Chen and J. J. Feng, *Biosens. Bioelectron.*, 2015, **64**, 517-522.

30. B.-X. Zhang, H. Gao and X.-L. Li, *New J. Chem.*, 2014, **38**, 4615-4621.

31. H. Ding, J. S. Wei and H. M. Xiong, *Nanoscale*, 2014, **6**, 13817-13823.

32. W. Wang, Y.-C. Lu, H. Huang, A.-J. Wang, J.-R. Chen and J.-J. Feng, *Sensor. Actuat. B*, 2014, **202**, 741-747.

33. H. Huang, Y.-C. Lu, A.-J. Wang, J.-H. Liu, J.-R. Chen and J.-J. Feng, *RSC Adv.*, 2014, **4**, 11872-11875.

34. Y.-C. Lu, J. Chen, A.-J. Wang, N. Bao, J.-J. Feng, W. Wang and L. Shao, *J. Mater. Chem. C*, 2015, **3**, 73-78.

35. J. R. Lakowicz, *Principles of Fluorescence Spectroscopy*, 2nd edn., Kluwer Academic/Plenum Publisher, 1999.

36. C.-H. Chang, L. S. Lico, T.-Y. Huang, S.-Y. Lin, C.-L. Chang, S. D. Arco and S.-C. Hung, *Angew. Chem. Int. Ed.*, 2014, **53**, 9876-9879.

37. J. Wei, X. Zhang, Y. Sheng, J. Shen, P. Huang, S. Guo, J. Pan, B. Liu and B. Feng, *New J. Chem.*, 2014, **38**, 906-909.

38. S. Zhu, J. Zhang, S. Tang, C. Qiao, L. Wang, H. Wang, X. Liu, B. Li, Y. Li, W. Yu, X. Wang, H. Sun and B. Yang, *Adv. Funct. Mater.*, 2012, **22**, 4732-4740.

39. J. Jiang, Y. He, S. Li and H. Cui, *Chem. Commun.*, 2012, **48**, 9634-9636.

40. J. P. Paraknowitsch, Y. Zhang, B. Wienert and A. Thomas, *Chem. Commun.*, 2013, **49**, 1208-1210.

41. K. Gong, F. Du, Z. Xia, M. Durstock and L. Dai, *Science*, 2009, **323**, 760-764.

42. S. Yang, L. Zhi, K. Tang, X. Feng, J. Maier and K. Müllen, *Adv. Funct. Mater.*, 2012, **22**, 3634-3640.

43. X. Li, S. P. Lau, L. Tang, R. Ji and P. Yang, *Nanoscale*, 2014, **6**, 5323-5328.

44. Z. Yang, M. Xu, Y. Liu, F. He, F. Gao, Y. Su, H. Wei and Y. Zhang, *Nanoscale*, 2014, **6**, 1890-1895.

45. G. Eda, Y. Y. Lin, C. Mattevi, H. Yamaguchi, H. A. Chen, I. S. Chen, C. W. Chen and M. Chhowalla, *Adv. Mater.*, 2010, **22**, 505-509.

46.   D. Wang, L. Wang, X. Dong, Z. Shi and J. Jin, *Carbon*, 2012, **50**, 2147-2154.

47.   H. Li, X. He, Y. Liu, H. Huang, S. Lian, S.-T. Lee and Z. Kang, *Carbon*, 2011, **49**, 605-609.

48.   J. Hou, J. Yan, Q. Zhao, Y. Li, H. Ding and L. Ding, *Nanoscale*, 2013, **5**, 9558-9561.

49.   P. Li, L. Huang, Y. Lin, L. Shen, Q. Chen and W. Shi, *Nanotechnology*, 2014, **25**, 055603-055608.

50.   T. Lai, E. Zheng, L. Chen, X. Wang, L. Kong, C. You, Y. Ruan and X. Weng, *Nanoscale*, 2013, **5**, 8015-8021.

51.   H. Zhu, X. Wang, Y. Li, Z. Wang, F. Yang and X. Yang, *Chem. Commun.*, 2009, **45**, 5118-5120.

52.   R.-J. Fan, Q. Sun, L. Zhang, Y. Zhang and A.-H. Lu, *Carbon*, 2014, **71**, 87-93.

53.   X. Zhai, P. Zhang, C. Liu, T. Bai, W. Li, L. Dai and W. Liu, *Chem. Commun.*, 2012, **48**, 7955-7957.

54.   S. Sahu, B. Behera, T. K. Maiti and S. Mohapatra, *Chem. Commun.*, 2012, **48**, 8835-8837.

55.   Y.-L. Zhang, L. Wang, H.-C. Zhang, Y. Liu, H.-Y. Wang, Z.-H. Kang and S.-T. Lee, *RSC Adv.*, 2013, **3**, 3733-3738.

56.   S. Zhang, J. Li, M. Zeng, J. Xu, X. Wang and W. Hu, *Nanoscale*, 2014, **6**, 4157-4162.

57.   D. Zarkowsky, L. Lamoreaux, P. Chattopadhyay, R. A. Koup, S. P. Perfetto and M. Roederer, *Cytom. Part A*, 2011, **79**, 84-89.